Ecosystem-specific patterns and drivers of global reactive iron mineral-associated organic carbon

Bo Zhao[1], Amin Dou[1], Zhiwei Zhang[1], Zhenyu Chen[1], Wenbo Sun[1], Yanli Feng[1], Xiaojuan Wang[2], Qiang Wang[1,*]

[1]*State Key Laboratory of Herbage Improvement and Grassland Agro-ecosystems, College of Pastoral Agriculture Science and Technology, Lanzhou University, Lanzhou 730000, China*

[2]*Natural History Research Center, Shanghai Natural History Museum, Shanghai Science & Technology Museum, 200127 Shanghai, China*

[*]**Corresponding author:** Qiang Wang (Phone: +86-136-6933-7869; Email: wqiang@lzu.edu.cn)

Type of paper: Research Paper; Text pages: 40; Figures: 7

Abstract

Reactive iron (Fe) oxides are vital for long-term soil/sediment organic carbon (SOC) storage. However, the patterns and drivers of Fe-associated organic carbon (Fe-OC) over global geographic scales under various ecosystem types remain controversial. Here, we provided a systematic assessment of the distribution patterns and determinants of Fe-OC content and its contribution to SOC (*f*Fe-OC) by assembling a global dataset comprising 862 observations from 325 sites in distinct ecosystems. We found that Fe-OC content across global ecosystems ranged from 0 to 83.3 g kg^{-1} (*f*Fe-OC ranged from 0 to 82.4%), reflecting the high variability of the Fe-OC pool. Fe-OC contents varied with ecosystem type, being greater in wetlands with a high molar ratio of Fe-OC/dithionite-extractable Fe (Fe_d) compared with marine and terrestrial ecosystems. Furthermore, *f*Fe-OC in wetlands was significantly lower than that in other ecosystems due to rich OC. In contrast with climate variables and soil pH, the random forest modelling and multivariate analysis showed that the Fe-OC:Fe_d and SOC were the predominant predictors of Fe-OC content and *f*Fe-OC in wetlands and terrestrial ecosystems, whereas Fe_d content was a primary driver in marine ecosystems. Based on upper estimates of global SOC storage in various ecosystem types, we further estimated that 83.84 ± 3.86 Pg, 172.45 ± 8.74 Pg, and 24.48 ± 0.87 Pg of SOC were preserved by association with Fe oxides in wetlands, terrestrial and marine ecosystems, respectively. Taken together, our findings highlighted the importance of reactive Fe oxides in global SOC preservation, and their controlling factors were ecosystem-specific.

Keywords: Ecosystem type, mineral protection, reactive iron oxides, iron-bound

35 organic carbon, organic carbon preservation

1. Introduction

The global soil (sediment) organic carbon (SOC) cycle has become one of the hotspots in biogeochemical and global climate change research (Lal, 2004a; Crowther et al., 2016). Organic carbon (OC) sequestration is a significant ecosystem service (such as climate mitigation, soil fertility and ecosystem stability, etc.) provided by terrestrial, wetland, and marine ecosystems. Accumulating evidence has shown that the reactive mineral matrix plays a critical role in sequestering and stabilizing SOC (Kramer and Chadwick, 2018; Ye et al., 2022). OC has a strong affinity for reactive Fe (hydr-)oxides (Longman et al., 2022), and the resulting Fe and OC association by adsorption or coprecipitation is thought to promote OC long-term preservation in soils and sediments (Schmidt et al., 2011; Hemingway et al., 2019). Therefore, a systematic understanding of the patterns and drivers of Fe-associated OC (Fe-OC) is pivotal for accurately predicting SOC dynamics and reducing model uncertainties in forecasting carbon-climate feedback at the global scale.

In comparison to other metal minerals, Fe (hydr-)oxides, one of the most prevalent reactive minerals, have larger specific surface areas, a higher OC affinity, and a greater potential to retain SOC (Guggenberger and Kaiser, 2003; Eusterhues et al., 2005; Kaiser et al., 2007). A growing body of studies has suggested that Fe (hydr-)oxides play a fundamental role in stabilizing SOC in sediment and soil (Yu et al., 2021). Recently, Fe-OC has been extracted and quantified through the bicarbonate-citrate-dithionite (BCD) method, and was estimated to constitute 21.5% (Lalonde et al., 2012), 4.7–37.8% (Zhao et al., 2016; Fang et al., 2019; Zong et al., 2021), and 3.4–11.8% (Huang et al.,

2021; Wang et al., 2021) of SOC in marine sediments, terrestrial (i.e., forests, grasslands, farmland) and wetlands (i.e., coastal, peatland, and lake wetlands), respectively. The Fe-OC content and contribution (*f*Fe-OC) vary with ecosystem type. Marine sediments are the largest OC sink on Earth and are crucial to the global carbon cycle. Reactive Fe minerals can protect and bury large amounts of SOC within marine sediments, constituting a "rusty sink" (Lalonde et al., 2012). The *f*Fe-OC in marine sediments is significantly lower than that in offshore estuarine sediments due to differences in sediment mineralogy, reactive Fe source and organic matter composition (Longman et al., 2022). It is well known that wetland ecosystems possess an extremely high rate of OC sequestration (McLeod et al., 2011; Hopkinson et al., 2012). Compared with terrestrial and marine ecosystems, wetland soils or sediments are periodically submerged due to (semi-)diurnal tidal cycles or fluctuations in the water table (Yu et al., 2021). Thus, in wetland environments, Fe (hydr-)oxides are repeatedly formed and destroyed as a result of periodical redox-induced changes in Fe^{2+}/Fe^{3+} (Patzner et al., 2020), which is thought to weaken the interaction between Fe and OC (Huang and Hall, 2017; LaCroix et al., 2019; Anthony and Silver, 2020). However, Wang et al. (2017) proposed an important "iron gate" mechanism in OC-rich wetlands (Wang et al., 2017), and showed that the *f*Fe-OC in wetlands and uplands is equally important (Wang et al., 2017). Thus, a systematic analysis of Fe-OC content and *f*Fe-OC in terrestrial, wetland and marine ecosystems at the global scale can provide evidence for the importance of reactive Fe minerals in global climate change.

Recently, some studies have found that the Fe-OC content and *f*Fe-OC are mainly

controlled by soil properties (Grybos et al., 2009; Ye et al., 2022), organic matter composition (Fisher et al., 2020), and climate (or latitude) (Kramer and Chadwick, 2018). For instance, Fe-OC increases with increasing latitude, mean annual precipitation (MAP), SOC content, and potential evapotranspiration (Zhao et al., 2016; Kramer and Chadwick, 2018), but it decreases with increasing soil pH at the continental scale (Ye et al., 2022). However, Fe-OC content and *f*Fe-OC in farmland soils are not related to latitude, mean annual temperature (MAT) and MAP but are related to SOC content (Wan et al., 2019). In peatlands, Huang et al. (2021) found that Fe-OC content is positively correlated with the SOC content, C:N, and MAT but not with MAP at the regional scale (Huang et al., 2021). However, Fe-OC in coastal wetlands was positively correlated with amorphous Fe content and clay content, but negatively correlated with soil pH and phenol oxidase activity (Bai et al., 2021). In marine sediments, Fe-OC content may be mainly responsible for SOC content and organic matter functional groups (especially carboxyl content) (Wang et al., 2019; Fisher et al., 2020). Additionally, according to Kramer & Chadwick (2018), *f*Fe-OC in humid climate forest regions was much higher than that in semiarid and arid regions, confirming the natural linkages between *f*Fe-OC and climate (Kramer and Chadwick, 2018). Fe-OC content is also influenced by the bonding mechanism of Fe and OC (Wagai and Mayer, 2007; Faust et al., 2021). The bonding mechanism between Fe and OC is determined by the Fe-OC/dithionite-extractable Fe (Fe_d) molar ratio (Faust et al., 2021; Wang et al., 2021), with less than 1 indicating an Fe-OC bonding form of monolayer surface sorption, and greater than 6 indicating a bonding mechanism dominated by coprecipitation (Wagai

and Mayer, 2007; Lalonde et al., 2012). Generally, the OC content of the complexes obtained by coprecipitation is much higher than that of adsorption (Chen et al., 2014), which may also explain the wide variations in Fe-OC and *f*Fe-OC. Thus, uncovering the factors controlling Fe-OC formation/association at the global scale is a prerequisite for predicting the size of the OC pool and its feedback on global climate change. However, the determinants of Fe-OC associations remain unknown globally, and only two studies on Fe-OC have been undertaken at continental scale, which focus on the relationships of Fe-OC and soil pH (Ye et al., 2022), MAP and potential evapotranspiration (Kramer and Chadwick, 2018). These studies overlooked the influence of climate and soil properties (such as soil pH, Fe_d, Fe-OC:Fe_d, clay content) in controlling Fe-OC and *f*Fe-OC in wetland and marine ecosystems. Furthermore, they have not yet explored the relationship between these key factors and Fe-OC and *f*Fe-OC across global ecosystem types. A deeper understanding of these limitations in terrestrial, wetland and marine ecosystems will allow us to draw clear conclusions regarding global patterns and drivers of Fe-OC.

In this study, we provide a comprehensive analysis of the spatial variability and characteristics of Fe-OC among terrestrial, wetland and marine ecosystems and its governing factors globally. Specifically, we analysed data from 862 observations from 46 published papers and the National Ecological Observatory Network (NEON) to explore (i) the importance of Fe-OC to SOC storage in wetland and marine ecosystems and its level compared with terrestrial ecosystem, (ii) whether the distribution patterns (i.e., spatial variability) of Fe-OC and the relationships between key factors and Fe-OC

differ among ecosystem types? (iii) The bonding mechanism of reactive Fe and OC in different ecosystem types, i.e., adsorption or coprecipitation?

2. Materials and methods

2.1 Study selection

The ecosystem types included terrestrial, wetland, and marine systems in this study. We conducted extensive literature searches on the Web of Science (https://www.webofscience.com) and China National Knowledge Resource Integrated databases, and searched for relevant research published from 2010 to August 2022. The appropriate studies were identified by the following search terms: ('reactive mineral' OR 'iron') AND ('bound' OR 'associated' OR 'stabilization' OR 'interaction' OR 'sequestration') AND ('organic carbon')) (Fig. S1). The following criteria must be met for inclusion in this study: (a) soil samples at 0-100cm depth must be collected from in situ observation data of wetlands (i.e., peatland, bog, fen, deltaic, lake wetland, mangrove wetland, and estuary wetland), forests (i.e., evergreen forest, and deciduous forest), grasslands (i.e., temperate grasslands and alpine grasslands), farmland (i.e., paddy field and crop), and marine ecosystems (i.e., marine and river sediments); (b) the contents of Fe-OC and Fe_d were measured using the BCD method in bulk soil; and (c) Fe-OC, Fe-OC/Fe_d molar ratio must be provided or could be calculated from the publications. In total, we compiled 862 data records from 46 published papers, along with 42 additional data collected from NEON. The dataset involved 325 sites, with latitudes between 25.22°S and 81.75°N and longitudes between 156.4°W and 174.4°E (Fig. 1). We also collected global data on SOC stocks in terrestrial, wetland and marine

ecosystems, respectively, which will allow us to further estimate Fe-OC stocks in different ecosystems.

2.2 Data assembly and collection

Data from published articles and NEON were assembled to construct the Fe-OC dataset. Site-specific data such as ecosystem type, MAP, MAT, latitude, longitude, clay, soil pH, SOC, Fe-OC, Fe_d, Fe-OC/Fe_d molar ratio, and *f*Fe-OC (calculated using the following equation: *f*Fe-OC (%) = Fe-OC/SOC×100%) were collected from each published paper; other details are shown in Figure S1. If the MAT and MAP are not reported, the data for each site shall be obtained from the WordClim database (http://www.worldclim.org.d). The data obtained from the WorldClim database is the average climate data from 1970 to 2000. All original data and average data were taken from the published articles' text, graphs, and tables. When data were presented graphically, the numerical data were digitized and extracted with the GetData Graph Digitizer (v4.4, http://www.getdata-graph-digitizer.com).

2.3 Statistical analysis

All data analyses were conducted using the R platform (v 4.1.2; https://www.r-project.org/). We used the Shapiro-Wilk test to determine the homogeneity of variances and the normal distribution of the data before using parametric methods. We used the Kruskal–Wallis test to determine significant differences among different ecosystems.

Hedges' g, a bias-corrected standardized mean difference, was used to measure effect size to account for the bias of ecosystem-scale Fe-OC associated with small

sample sizes (Chien & Krumins, 2022; Smale et al., 2020). Based on ecosystem types, all data were divided into terrestrial, marine and wetland ecosystems, and the data were averaged separately for each ecosystem, representing 'control'. The sample sizes of individual cases (i.e., a single published article) represent 'treatment'. The standardized mean difference between the 'control' and 'treatment' was measured by the pooled variance (Chien & Krumins, 2022). We used the package "metafor" in R (v 4.1.2; https://www.r-project.org/) to generate forest plots for every ecosystem by using a random effects model (Fig. S2). We calculated the total observed change (I^2) and used heterogeneity test (Q) to verify the heterogeneity of the collected data, and an I^2 value higher than 75% or $p < 0.05$ indicates substantial heterogeneity (Meisner et al., 2014). We performed Spearman's correlation analyses to evaluate the relationship between environmental variables (SOC, MAT, MAP, clay, soil pH, Fe-OC:Fe_d, Fe_d, and latitude) and Fe-OC and *f*Fe-OC. The linear ("lm" function in R) fitting was demonstrated to analyse the relationships between environmental variables and Fe-OC and *f*Fe-OC. The significant correlation was considered at $p < 0.05$. To test the relative importance of these drivers, a random forest analysis (RF, Breiman, 2001) was performed according to the protocol described by Delgado-Baquerizo et al. (2016). For the RF analyses, the climate variables (MAT, MAP), soil properties (SOC, clay, soil pH, Fe-OC:Fe_d, and Fe_d), and geographical location (i.e., latitude) were involved as predictors, and the Fe-OC and *f*Fe-OC changes and dynamics as the response variables. The significance of the models and cross-validated R^2 values were evaluated with 500 permutations of the response variables with the "A3" R package. Similarly, using the "rfPermute" package

for R (p < 0.05), the importance of each predictor on the response variables was evaluated.

3. Results

3.1 Fe-associated OC and its related indicators across ecosystem types

Across global ecosystem types (i.e., terrestrial, wetland and marine ecosystems), Fe-OC content (n = 862) and *f*Fe-OC (n = 855) varied significantly and ranged from 0 to 83.3 mg g^{-1} (mean: 5.62 ± 0.32 mg g^{-1}) and 0–82.4% (mean: 16.03 ± 0.41%), respectively (Figs. 2a, b). The contents of Fe-OC in terrestrial, marine and wetland ecosystems were 5.42 ± 0.41 mg g^{-1} (*f*Fe-OC: 17.76 ± 0.90%), 2.34 ± 0.12 mg g^{-1} (*f*Fe-OC: 16.32 ± 0.58%) and 9.97 ± 0.91 mg g^{-1} (*f*Fe-OC: 13.70 ± 0.63%), respectively, with significant differences among ecosystem types (p < 0.05; Fig. 2a). Correspondingly, the contribution of Fe-OC to SOC (*f*Fe-OC) was significantly different among different ecosystem types (p < 0.05; Fig. 2b). Meanwhile, Hedges' g unbiased standardized mean difference showed that small sample sizes at local scale (i.e., single published articles) had obvious distinct effect sizes for ecosystem-scale Fe-OC (I^2 > 75% or p < 0.05), especially for marine ecosystems (Fig. S2). Fe_d contents (n = 856) ranged from 0.03 to 245 mg g^{-1} (mean: 9.43 ± 0.53 mg g^{-1}; Fig. 2c); that is, Fe_d varied 8167-fold, which was significantly higher in terrestrial ecosystems than in wetland and marine ecosystems (p < 0.05; Fig. 2c). The Fe-OC/Fe_d molar ratio (n = 855) ranged from 0–331.68 (mean: 8.40 ± 0.85) at the global scale, and its mean value was significantly higher in wetlands than in terrestrial systems, while the minimum value was found in marine systems (p < 0.05; Fig. 2d). SOC contents (n = 854) ranged

211 from 0.3 to 423.74 mg g^{-1} (mean: 43.28 ± 2.52 mg g^{-1}), which had similar changes with
212 the Fe-OC contents among ecosystem types ($p < 0.05$; Fig. 2e). Taken together, the Fe-
213 OC, SOC, and Fe-OC/Fe_d molar ratio were significantly higher in wetlands, with the
214 lowest values in marine ecosystems across global ecosystem types.

215 **3.2. Effect of environmental factors on Fe-OC and *f*Fe-OC across ecosystem types**

216 We analysed their relationships with climate variables and soil properties to better
217 understand the potential effect factors behind the observed variance in Fe-OC contents
218 and *f*Fe-OC among ecosystem types (Fig. 3). Among them, in wetland ecosystems, Fe-
219 OC content showed a negative correlation with MAT (R = -0.42, $p < 0.001$; Fig. 3a) and
220 MAP (R = -0.26, $p < 0.001$; Fig. 3b), while *f*Fe-OC was positively correlated with the
221 climate variables (MAT, MAP) (Figs. 3i, j). The Fe-OC content decreased significantly
222 with increasing soil pH in wetlands (R = -0.24, $p < 0.01$; Fig. 3c) and terrestrial systems
223 (R = -0.19, $p < 0.05$; Fig. 3c), but *f*Fe-OC increased with increasing soil pH (R = 0.52,
224 $p < 0.001$; Fig. 3k) in wetlands. Across the ecosystem types, Fe_d contents showed
225 positive correlations with Fe-OC (R = 0.25, p <0.001; Fig. 3g) and *f*Fe-OC (R = 0.28,
226 $p < 0.001$; Fig. 3o) in marine ecosystems only. Moreover, Fe-OC increases significantly
227 with Fe_d contents (R = 0.35, $p < 0.001$; Fig. 3g) in wetlands, but *f*Fe-OC does not;
228 however, Fe_d content has no relationship with Fe-OC and *f*Fe-OC in terrestrial
229 ecosystems. The molar ratio of Fe-OC/Fe_d was positively correlated with Fe-OC and
230 *f*Fe-OC in other ecosystems, except for *f*Fe-OC which not correlated with the molar
231 ratios in wetlands (Figs. 3e, m). Fe-OC contents increased significantly, but *f*Fe-OC
232 (except marine) decreased with increasing SOC contents in all ecosystems (Figs. 3f, n).

At continental scales, Fe-OC content (R = 0.35, p < 0.001; Fig. 3d) and fFe-OC (R = 0.44, p < 0.001; Fig. 3l) were positively related to clay content. Latitudinal patterns in Fe-OC content and fFe-OC were observed across global ecosystem types (Figs. 3h, p). Taken together, Fe-OC contents are significantly correlated with both SOC and the Fe-OC/Fe_d molar ratio, which may be important predictors of Fe-OC in global ecosystems.

Moreover, according to RF analysis, the Fe-OC/Fe_d molar ratio and SOC and Fe_d contents were found to be the most important variables for predicting the Fe-OC content and fFe-OC across global ecosystem types (Fig. 4). Different controlling factors on Fe-OC content and fFe-OC were operational among ecosystem types. At continental scales, the Fe-OC/Fe_d molar ratio was a central driver of the Fe-OC content and fFe-OC, and the contents of SOC and Fe_d had a more significant influence than the soil pH and climate variables (MAT, MAP) (Figs. 4a, b). The largest influence on Fe-OC content and fFe-OC in marine ecosystem was in the order of Fe_d > Fe-OC:F_d > SOC > latitude (Figs. 4c, d). In wetlands, the Fe-OC/Fe_d molar ratio was the main driver of Fe-OC, whereas SOC had a more significant role than Fe_d and soil pH (Fig. 5e); For fFe-OC, the largest influence was in the range of SOC > Fe-OC:F_d > pH > MAT > MAP > Fe_d (Fig. 4f). The role of Fe_d content in controlling Fe-OC content and fFe-OC was greater in marine systems than in terrestrial and wetland systems. These results revealed that drivers of both Fe-OC content and fFe-OC were ecosystem specific. The climate predictors accounted for relatively small percentages in all ecosystems. Collectively, Fe-OC:F_d, SOC, and Fe_d were all selected by RF analysis as important predictors of changes in Fe-OC content and fFe-OC, which agreed with the results of our Spearman's

correlation analyses (Fig. 3).

3.3. The vital role of Fe-OC:Fe_d in controlling Fe/OC interactions

At the continental scale, the proportions of Fe-OC/Fe_d molar ratios less than 1 (< 1), between 1 and 6 (1–6), and higher than 6 (> 6) were 33.10%, 47.89%, and 19.01%, respectively (Fig. 5). Moreover, we found that the proportions of 1–6 were larger in grasslands and farmland than in forests, but the proportions of > 6 in grasslands were higher. In marine ecosystems, the proportion of Fe-OC:Fe_d < 1 (31.0%) is lower than that of 1–6 (63.75%), and the proportion of > 6 (5.31%) is the smallest. However, the proportion of Fe-OC:Fe_d > 6 (39.44%) in wetlands was significantly higher than that in other ecosystems (19.01% and 5.31%, respectively), but the proportion of <1 (13.55%) was lower.

Consistent with our expectation, the molar ratio was significantly positively correlated with Fe-OC and SOC contents but negatively correlated with Fe_d in all ecosystem types (Fig. 6). Moreover, the results showed that MAT and MAP are also major negative regulators of the molar ratio dynamics at the continental scale, whereas in wetlands, it is soil pH (Figs. 6a, c).

4. Discussion

4.1 Reactive Fe promotes SOC preservation at the global scale

In contrast to previous studies (Kramer and Chadwick, 2018; Yu et al., 2021; Ye et al., 2022), our findings suggested that a comprehensive analysis of global patterns of Fe-OC associations across ecosystem types, particularly in wetland and marine

ecosystems, can bridge the knowledge gap in understanding the importance of global SOC preservation by reactive Fe. Generally, mineral-associated organic carbon is the dominant SOC pool in soil systems, with a proportion of approximately 50–80% of SOC (Cotrufo et al., 2019). As an important component of reactive minerals, Fe (hydr-)oxides play a fundamental role in the formation and dynamics of mineral-associated organic carbon (Lalonde et al., 2012). Our findings showed that the average content of Fe-OC was 5.63 ± 0.32 mg g^{-1} soil (n = 862), and the proportion (*f*Fe-OC) of Fe-OC in total SOC was 16.03 ± 0.41% (n = 855) across global ecosystems (Figs. 2a, b), indicating that Fe-OC is essential to the persistence of SOC. Consistent with our expectation, the *f*Fe-OC of wetlands is significantly lower than that of marine and terrestrial systems. At the continental scale, the mean *f*Fe-OC was 17.75 ± 0.90% (0–82.36%, n = 284), which was consistent with findings from Tibetan alpine meadows (15.8 ± 12.0%) (Fang et al., 2019) but was lower than those for continental-scale forests, such as moist forests (25.3–49.8%) and wet forests (47.1–64.1%) (Zhao et al., 2016; Kramer and Chadwick, 2018). According to upper estimates of global terrestrial SOC storage (971 Pg) (including forest (383 Pg), grassland (423 Pg) and farmland (165 Pg)) (Carter et al., 2000; Lal, 2004b; Pan et al., 2011; Prentice et al., 2001), we estimated that 172.45 ± 8.74 Pg of SOC was bound to Fe oxides in terrestrial ecosystems. Meanwhile, we predicted that 49.02 ± 5.24 Pg (12.80 ± 1.37%), 74.28 ± 4.95 Pg (17.56 ± 1.17%), and 28.41 ± 4.34 Pg (17.22 ± 2.63%) of SOC were associated with Fe oxides in forests, grasslands, and farmlands, respectively. In contrast to terrestrial ecosystems, evidence of interactions between Fe and SOC in marine

298 sediments has been reported more often (Berner, 1970), but the potentially importance
299 of reactive Fe for SOC preservation has only recently been recognized in marine
300 sediments (Lalonde et al., 2012). Recently, an accumulating body of studies have
301 shown that reactive Fe has a strong affinity for SOC, forming stable Fe-OC complexes
302 that can persist for thousands of years in marine sediments, serving as a "rusty sink"
303 for marine sedimentary carbon (Lalonde et al., 2012; Faust et al., 2021). Our findings
304 suggested that *f*Fe-OC in global marine sediments ranged widely from 0.51% to
305 60.3%, with a mean of 16.32 ± 0.58%. These values are consistent with published
306 estimates for the East China Sea (13.2 ± 8.9%) (Ma et al., 2018), Bohai Sea (11.5 ±
307 8.3%) (Wang et al., 2019), River Delta (8.1–20.2%) (Shields et al., 2016), Barents Sea
308 (10–20%) (Faust et al., 2021), and global marine surface sediments (21.8 ± 8.6%)
309 (Lalonde et al., 2012). Based on model-predicted global marine sedimentary OC
310 stocks (150 Pg) (Hedges & Keil, 1995), we further estimated that 24.48 ± 0.87 Pg of
311 the marine sedimentary OC was directly associated with Fe oxides, which was
312 comparable to the results of previous study (19–45 Pg OC) (Lalonde et al., 2012).
313 Wetland ecosystems, however, frequently experience seawater flooding, atmosphere
314 exposure, and/or disruption of the hydrological balance due to (semi)diurnal tidal
315 cycles or water table drawdown, in contrast to terrestrial and marine systems (Huang
316 and Hall, 2017; Patzner et al., 2020). Fe-OC associations are weakened with the
317 reductive breakdown of Fe(III) (hydr)oxides driven by periodic soil redox processes
318 (Patzner et al., 2020). Although wetlands store 20–30% of the Earth's soil carbon
319 (~2500 Pg) (Roulet, 2000; Bridgham et al., 2006), the importance of Fe-OC in wetland

soils/sediments remains controversial. In global wetlands, we found that the absolute content of Fe-OC was significantly higher than those in terrestrial and marine ecosystems, whereas the opposite was true for *f*Fe-OC, which was significantly lower in wetlands. Our findings in wetlands were also consistent with those of Ye et al. (2022) at continental scales (13.6 ± 1.0%; Ye et al., 2022) and regional-scale wetlands (16.1 ± 1.4%) (Wang et al., 2021) but were higher than those for specific peatland ecosystems (3.42 ± 1.32%) (Huang et al., 2021). Compared with coastal wetlands (for instance, mangrove wetland and tidal wetland) (Bai et al., 2021; Zhao et al., 2022), inland wetlands (for instance, alpine wetland and peatland) have lower *f*Fe-OC (Wang et al., 2017; Huang et al., 2021), which may lead to significantly lower *f*Fe-OC in global wetlands. Therefore, the significance of reactive Fe minerals for SOC sequestration in global wetlands may be underestimated based on peatland *f*Fe-OC (Huang et al., 2022). Here, based on global wetland *f*Fe-OC and total SOC stocks (612 Pg) (Yu et al., 2010), we predicted that 83.84 ± 3.86 Pg of SOC was preserved by binding to Fe oxides. Collectively, these findings confirmed the fundamental role of reactive Fe minerals for OC sequestration and conservation in global ecosystems.

Two possible mechanisms may explain the higher Fe-OC content in wetlands than in other ecosystems. First, the molar ratios of Fe-OC:Fe_d were significantly higher in wetlands than in terrestrial and marine ecosystems ($p < 0.05$; Fig. 2d), suggesting that in wetlands reactive Fe is more effective in OC binding (Wagai and Mayer, 2007; Riedel et al., 2013). Numerous studies have shown that the Fe-OC:Fe_d acts as an indicator of Fe/OC interaction types (Lalonde et al., 2012; Wang et al., 2017), with <1 suggesting

that the Fe-OC bonding form is dominated by simple mono-layer adsorption, while higher molar ratios (>6) indicating coprecipitation (Wagai and Mayer, 2007; Faust et al., 2021). Thus, compared with other ecosystems, in wetlands coprecipitation played a more significant role in the binding/association of Fe-OC. Second, the SOC content in wetlands was significantly higher than that in terrestrial and marine ecosystems ($p < 0.05$; Fig. 2e), and it is generally believed that the SOC in wetlands has various chemical bonds or chemical compositions (Wang et al., 2017; Coward et al., 2018). Thus, the high SOC content in wetlands could be responsible for the predominance of Fe(II) with a strong OC-complexation capacity (Jones et al., 2015; Bhattacharyya et al., 2018; Patzner et al., 2022), especially the enrichment of phenolic (Freeman et al., 2001), ultimately promoting the Fe-OC association (Riedel et al., 2013; Coward et al., 2018).

4.2 Ecosystem-specific relationships of Fe-OC associations with key factors

The role of soil pH, SOC, Fe_d, Fe-OC:Fe_d, MAT and MAP in controlling Fe-OC contents and *f*Fe-OC among ecosystem types was thoroughly analysed. A compilation of global datasets including terrestrial, wetland, and marine ecosystems demonstrated that Fe-OC content and *f*Fe-OC are strongly coupled to both the Fe-OC:Fe_d molar ratio and SOC content ($p < 0.001$; Figs. 3e, f, m, n), indicating that the two variables are important determinants of Fe-OC content and *f*Fe-OC. The results from the RF models also revealed that Fe-OC:Fe_d molar ratio, SOC content, and Fe_d content were important predictors of Fe-OC and *f*Fe-OC across ecosystem types (Fig. 4). Collectively, these findings suggested a generic dependency of Fe-OC and *f*Fe-OC on the Fe-OC:Fe_d molar ratio and SOC, regardless of their ecosystem types. Former studies on the

response of Fe-OC to climate variables and soil properties only concentrated on the continental scale and specific ecosystems with limited data (Ye et al., 2022), making it challenging to reach definitive conclusions. Kramer & Chadwick (2018) concluded that continental-scale Fe-OC variation depended on MAP and potential evapotranspiration but overlooked the role of soil properties (Kramer and Chadwick, 2018). Our findings further showed that the soils with higher MAP were linked with lower soil pH (Fig. 6), which had a positive effect on Fe-OC contents at the continental scale (Fig. 3c), and these results are in line with Ye et al. (2022) (Ye et al., 2022). Furthermore, we found that Fe-OC content was primarily controlled by the Fe-OC:Fe_d molar ratio at the continental scale and wetlands (Fig. 7). Given the strong affinity of OC with [Fe(III)] (hydr-)oxides, we speculated that an increase in Fe_d content would lead to higher Fe-OC content, assuming sufficient SOC was present (Ma et al., 2018; Wang et al., 2019). Although reactive Fe plays a fundamental role in OC binding, its content is not related to Fe-OC content in specific terrestrial ecosystems, such as the Qinghai-Tibet Plateau and regional-scale forests (Mu et al., 2016; Zhao et al., 2016). Our study, for the first time, illustrated the crucial role of Fe_d in controlling Fe-OC contents and fFe-OC in global marine ecosystems (Fig. 3g and Fig. 4c). Previous findings indicated that increased terrigenous reactive Fe inputs contributed to higher Fe-OC contents (Ma et al., 2018; Wang et al., 2019). Therefore, sedimentary Fe_d content was the controlling factor of Fe-OC associations in marine ecosystems. The findings of Faust et al. (2021), however, who showed that a higher Fe_d content does not always enhance Fe-OC associations in Arctic marine sediments, were in contrast to our findings (Faust et al.,

2021). The differences between our results and those of Arctic marine sediments may be mainly related to the study scale. Nevertheless, the bonding mechanism of Fe and OC (adsorption vs. coprecipitation) is a predominant driver of *f*Fe-OC in wetlands and terrestrial ecosystems, as illustrated by the RF analysis and a good linear correlation. Given that the Fe and OC interactions are substantially controlled by Fe redox processes (Riedel et al., 2013; Adhikari et al., 2016), we posited that the contents and proportions of Fe-OC are governed mainly by Fe redox cycling and associated bonding mechanisms, with the exception of the marine ecosystems. The results of this study suggested that future climate warming may increase the proportions of Fe-OC in the total SOC, especially in wetlands (Figs. 3i, j), even though additional research is necessary to fully understand the effects of climate changes on Fe-OC at the global scale.

4.3 Potential bonding mechanism between Fe and OC across ecosystem types

Adsorption and coprecipitation are well-known to be important and well-documented processes for the association of OC and reactive Fe (Lalonde et al., 2012; Chen et al., 2014). Reactive Fe can act as sorbents of OC to adsorb large amounts of OC to mineral surfaces due to its ubiquity in the environment, high surface area and small particle size (Kaiser and Guggenberger, 2003). Riedel et al. (2013) showed that coprecipitated Fe-OC complexes form when reduced Fe is oxidized in the presence of dissolved OC at the oxic-anoxic interface and present a high Fe-OC:Fe_d molar ratio (Riedel et al., 2013). The Fe-OC:Fe_d molar ratio can be used as an indicator for the bonding mechanism between Fe and OC (Lalonde et al., 2012; Peter and Sobek, 2018; Faust et al., 2021; Wang et al., 2021), with <1 indicating simple mono-layer sorption

and >6 indicating coprecipitation (Tipping et al., 2002; Wagai and Mayer, 2007). Our findings suggested that the average Fe-OC:Fe_d molar ratio was 10.50 ± 1.91 at the continental scale. However, we could see that the Fe-OC:Fe_d molar ratios (mean 70.18 ± 13.82; range 2.58–331.68) were much higher in permafrost regions of the Tibetan Plateau than in other specific terrestrial ecosystems, resulting from relatively high Fe-OC and low Fe_d (Mu et al., 2016). In view of the very high molar ratio, coprecipitation is the dominant bonding mechanism of OC and Fe, which contributes to *f*Fe-OC reaching 59.5% (average 19.5 ± 12.3%) in Fe-poor (range 0.03−2.68 mg g^{-1} soil) permafrost soils of the Tibetan Plateau (Mu et al., 2016). If the permafrost region of the Tibetan Plateau is excluded, the Fe-OC:Fe_d molar ratio in global terrestrial ecosystems was only 3.74 ± 0.47, indicating that coprecipitation will become a less important bonding mechanism. Recently, a regional-scale survey including typical grasslands, shrublands and forests by Wang et al. (2021) reported that the average Fe-OC:Fe_d molar ratio was 3.0 ± 0.5 (Wang et al., 2021), which lends further credence to the findings mentioned above. The average Fe-OC:Fe_d molar ratio was 2.56 ± 0.19 (n = 320) in global marine ecosystems, similar to that of the Bohai Sea (1.59 ± 1.37) (Wang et al., 2019), Southern Yellow Sea (1.68 ± 1.80) (Ma et al., 2018), East China Sea (1.53 ± 1.28) (Ma et al., 2018), and Barents Sea (2.56 ± 1.76) (Faust et al., 2021), but was much lower than the previous average of global oceans (6.10 ± 7.5) (Lalonde et al., 2012), Arctic shelf (Salvadó et al., 2015), and river delta (Shields et al., 2016) (Table S1). Moreover, in wetlands, the molar ratios of Fe-OC:Fe_d were higher (13.47 ± 1.81) than those in terrestrial and marine ecosystems. These results were in accordance with

previous findings in regional-scale wetlands (12.78 ± 2.43) (Wang et al., 2021) and coastal wetlands (11.0 ± 4.5) (Bai et al., 2021) but higher than that peatlands (mean 6.53) (Huang et al., 2021) (Table S1). This suggested that the interaction between OC and Fe in wetland ecosystems is mainly dominated by coprecipitation at the global scale, with a molar ratio of >6 usually. Overall, across the global ecosystem types, the average proportion of Fe-OC:Fe_d > 1 ranged from 60 to 80% (Fig. 5), which indicated the importance of both adsorption and coprecipitation interactions. Furthermore, we found that SOC content could enhance the molar ratio of Fe-OC:Fe_d by positively regulating Fe-OC content. At the continental scale, climate variables (MAT, MAP) can negatively regulate the molar ratio by changing the Fe_d content (Fig. 6a), while in wetlands, soil pH changes the Fe-OC content and then negatively regulates the molar ratio (Fig. 6c). Despite the molar ratio being widely used as an important indicator of the bonding mechanism of Fe and OC, recent studies have shown that only a portion of reactive Fe (25.7–62.6%) was directly associated with OC (Barber et al., 2017). Thus, using the raw Fe-OC:Fe molar ratio may result in an underestimation of the actual molar ratio due to the existence of OC-free Fe_d (Wang et al., 2019; Faust et al., 2021). At neutral to alkaline pH, associated with arid and semiarid soils, the association of reactive Fe and OC is limited (Sowers et al., 2018a; Sowers et al., 2018b), while calcium (Ca) is especially important in OC binding via Ca bridging (Sowers et al., 2018a; Wang et al., 2021). Wang et al. (2021) provided direct evidence that the Fe-OC determined by the classic BCD method contained Ca-bound OC, accounting for approximately 24% of Fe-OC (Wang et al., 2021), and the Fe-OC:Fe_d molar ratio might, therefore, be

overestimated, for example, in the permafrost regions of the Tibetan Plateau (soil pH 8.01–9.52) (Mu et al., 2016). Therefore, to draw a valid inference on the bonding mechanisms of OC and reactive Fe, further work is necessary to unravel the complex mechanisms.

5. Conclusions

To our knowledge, this is the first study to reveal the patterns and drivers of Fe-OC across global ecosystems (Fig. 7). More importantly, our global-scale results showed that Fe-OC was an important fraction of SOC at the continental scale, in wetlands, and in marine ecosystems. Our findings highlighted that some drivers for Fe-OC associations are valid globally, but those ecosystem-specific predictors should also be uncovered. Correlation analysis and RF modelling indicated that the Fe-OC:Fe_d molar ratio and SOC were the predominant predictors of Fe-OC and *f*Fe-OC compared with climate variables and soil pH in global ecosystems. The Fe-OC:Fe_d molar ratio was the predominant driver of Fe-OC at the continental scale and in wetlands, whereas Fe_d content was a good predictor in the global marine ecosystem, improving our ability to predict Fe-OC variations among ecosystem types. Moreover, in global wetlands, the fractions of Fe-OC in total SOC may be increasing in response to climate warming. As an indicator of the Fe and OC bonding mechanism, the molar ratio between 1–6 (<1 for adsorption, >6 for coprecipitation) in global ecosystems exceeds 60%, highlighting the importance of the interactions of both adsorption and coprecipitation. Compared with terrestrial and marine ecosystems, coprecipitation plays a more important role in wetlands due to the high molar ratio. Our findings provide direct evidence that reactive

Fe minerals are a dominant natural mechanism for long-term SOC storage in global ecosystems.

Acknowledgments

We are very grateful to all the researchers whose data were compiled in this study. This study was supported by the National Natural Science Foundation of China (32101333).

Conflict of interest

The authors declare that they have no known competing financial interests or personal relationships that could have appeared to influence the work reported in this paper.

Data availability statement

The data that supports the findings of this study are available in the Supporting Data Set.

References

Adhikari, D., Poulson, S. R., Sumaila, S., Dynes, J. J., McBeth, J. M., and Yang, Y.: Asynchronous reductive release of iron and organic carbon from hematite–humic acid complexes, Chem. Geol., 430, 13-20, https://doi.org/10.1016/j.chemgeo.2016.03.013,2016

Anthony, T. L., and Silver, W. L.: Mineralogical associations with soil carbon in managed wetland soils, Global Change Biol., 26, 6555-6567, https://doi.org/10.1111/gcb.15309,2020.

Bai, J., Luo, M., Yang, Y., Xiao, S., Zhai, Z., and Huang, J.: Iron-bound carbon increases along a freshwater-oligohaline gradient in a subtropical tidal wetland, Soil Biol. Biochem., 154, 108128, https://doi.org/10.1016/j.soilbio.2020.108128, 2021.

Barber, A., Brandes, J., Leri, A., Lalonde, K., Balind, K., Wirick, S., Wang, J., and Gelinas, Y.: Preservation of organic matter in marine sediments by inner-sphere interactions with reactive iron, Sci. Rep., 7, 366, https://doi.org/10.1038/s41598-017-00494-0,2017.

Berner, R. A.: Sedimentary pyrite formation, Am. J. Sci., 268, 1-23. https://doi.org/10.2475/ajs.268.1.1,1970.

Bhattacharyya, A., Campbell, A. N., Tfaily, M. M., Lin, Y., Kukkadapu, R. K., Silver, W. L., Nico, P. S., and Pett-Ridge, J.: Redox fluctuations control the coupled cycling of iron and carbon in tropical forest soils, Environ. Sci. Technol., 52, 14129-14139, https://doi.org/10.1021/acs.est.8b03408,2018.

Bridgham, S. D., Megonigal, J. P., Keller, J. K., Bliss, N. B., and Trettin, C.: The carbon balance of North American wetlands, Wetlands, 26, 889-916, https://doi.org/10.1023/A:1010933404324, 2006.

Carter, A. J., and Scholes, R. J.: Spatial global database of soil properties. In: IGBP Global Soil Data Task (Database on CD-ROM), International Geosphere-Biosphere Programme (IGBP) Data Information Systems, producer. Toulouse: IGBP, 2000.

Chen, C., Dynes, J. J., Wang, J., and Sparks, D. L.: Properties of Fe-organic matter associations via coprecipitation versus adsorption, Environ. Sci. Technol., 48, 13751-13759, https://doi.org/10.1021/es503669u,2014.

Chien, S.C., and Krumins, J. A.: Natural versus urban global soil organic carbon stocks: A meta-analysis, Sci. Total Environ., 807, 150999, https://doi.org/10.1016/j.scitotenv.2021.150999,

2022.

Cotrufo, M. F., Ranalli, M. G., Haddix, M. L., Six, J., and Lugato, E.: Soil carbon storage informed by particulate and mineral-associated organic matter, Nat. Geosci., 12, 989-994, https://doi.org/10.1038/s41561-019-0484-6,2019.

Coward, E. K., Thompson, A., Plante, A. F.: Contrasting Fe speciation in two humid forest soils: Insight into organomineral associations in redox-active environments, Geochim. Cosmochim. Ac., 238, 68-84, https://doi.org/10.1016/j.gca.2018.07. 007,2018.

Crowther, T. W., Todd-Brown, K. E., Rowe, C. W., et al.: Quantifying global soil carbon losses in response to warming, Nature, 540, 104-108, https://doi.org/10.1038/ nature20150,2016.

Delgado-Baquerizo, M., Grinyer, J., Reich, P. B., and Singh, B. K.: Relative importance of soil properties and microbial community for soil functionality: insights from a microbial swap experiment, Funct. Ecol., 30, 1862-1873, https://doi.org/10.1111/ 1365-2435.12674,2016.

Eusterhues, K., Rumpel, C., Kogel-Knabner, I.: Organo-mineral associations in sandy acid forest soils: importance of specific surface area, iron oxides and micropores, Eur. J. Soil Sci., 56, 753-763, https://doi.org/10.1111/j.1365-2389.2005.00710.x, 2005.

Fang, K., Qin, S., Chen, L., Zhang, Q., Yang, Y.: Al/Fe mineral controls on soil organic carbon stock across tibetan alpine grasslands, J. Geophys. Res-Biogeo., 124, 247-259, https://doi.org/ 10.1029/2018JG004782,2019.

Faust, J. C., Tessin, A., Fisher, B. J., Zindorf, M., Papadaki, S., Hendry, K. R., Doyle, K. A., and Marz, C.: Millennial scale persistence of organic carbon bound to iron in Arctic marine sediments, Nat. Commun., 12, 275, https://doi.org/10.1038/ s41467-020-20550-0,2021.

Fisher, B. J., Moore, O. W., Faust, J. C., Peacock, C. L., and März, C.: Experimental evaluation of the extractability of iron bound organic carbon in sediments as a function of carboxyl content, Chem. Geol., 556, 119853, https://doi.org/10.1016/ j.chemgeo.2020.119853,2020.

Freeman, C., Ostle, N., and Kang, H.: An enzymic 'latch' on a global carbon store, Nature, 409, 149-149, https://doi.org/10.1038/35051650,2001.

Grybos, M., Davranche, M., Gruau, G., Petitjean, P., and Pédrot, M.: Increasing pH drives organic matter solubilization from wetland soils under reducing conditions, Geoderma, 154, 13-19, https://doi.org/10.1016/j.geoderma.2009.09.001,2009.

544 Guggenberger, G., and Kaiser, K.: Dissolved organic matter in soil: challenging the paradigm of
545 sorptive preservation, Geoderma, 113, 293-310, https://doi.org/ 10.1016/S0016-
546 7061(02)00366-X,2003.
547 Hemingway, J. D., Rothman, D. H., Grant, K. E., Rosengard, S. Z., Eglinton, T. I., Derry, L. A., and
548 Galy, V. V.: Mineral protection regulates long-term global preservation of natural organic
549 carbon, Nature, 570, 228-231, https://doi.org/10.1038/s41586-019-1280-6,2019.
550 Hopkinson, C. S., Cai, W. J., and Hu, X.: Carbon sequestration in wetland dominated coastal
551 systems—a global sink of rapidly diminishing magnitude, Curr. Opin. Env. Sust., 4, 186-194,
552 https://doi.org/10.1016/j.cosust. 2012.03.005,2012.
553 Huang, W., and Hall, S. J.: Elevated moisture stimulates carbon loss from mineral soils by releasing
554 protected organic matter, Nat. Commun., 8, 1-10, https://doi.org/ 10.1038/s41467-017-01998-
555 z,2017.
556 Huang, X., Liu, X., Liu, J., Chen, H.: Iron-bound organic carbon and their determinants in peatlands
557 of China, Geoderma, 391, https://doi.org/10.1016/j.geoderma.2021. 114974,2021.
558 Jones, A.M., Griffin, P.J., Waite, T.D.: Ferrous iron oxidation by molecular oxygen under acidic
559 conditions: The effect of citrate, EDTA and fulvic acid, Geochim. Cosmochim. Ac., 160, 117-
560 131, https://doi.org/10.1016/j.gca.2015.03.026, 2015.
561 Kaiser, K., and Guggenberger, G.: Mineral surfaces and soil organic matter, Eur. J. Soil Sci., 54,
562 219-236, https://doi.org/10.1046/j.1365-2389. 2003.00544.x,2003.
563 Kaiser, K., Mikutta, R., and Guggenberger, G.: Increased stability of organic matter sorbed to
564 ferrihydrite and goethite on aging, Soil Sci. Soc. Am. J., 71, 711-719, https://doi.org/10.2136
565 /sssaj2006.0189,2007.
566 Kramer, M.G., and Chadwick, O.A.: Climate-driven thresholds in reactive mineral retention of soil
567 carbon at the global scale, Nat. Clim. Change, 8, 1104-1108, https://doi.org/10.1038/s41558-
568 018-0341-4,2018.
569 LaCroix, R.E., Tfaily, M.M., McCreight, M., Jones, M.E., Spokas, L., and Keiluweit, M.: Shifting
570 mineral and redox controls on carbon cycling in seasonally flooded mineral soils,
571 Biogeosciences, 16, 2573-2589, https://doi.org/10.5194/bg-16-2573-2019,2019.
572 Lal, R.: Soil carbon sequestration impacts on global climate change and food security, Science, 304,

573 1623-1627, https://doi.org/10.1126/science.1097396,2004a.
574 Lal, R.: Soil carbon sequestration to mitigate climate change, Geoderma, 123, 1-22,
575 https://doi.org/10.1016/j.geoderma.2004.01.032,2004b.
576 Lalonde, K., Mucci, A., Ouellet, A., and Gelinas, Y.: Preservation of organic matter in sediments
577 promoted by iron, Nature, 483, 198-200, https://doi.org/10.1038/ nature10855,2012.
578 Longman, J., Faust, J.C., Bryce, C., Homoky, W.B., März, C.: Organic carbon burial with reactive
579 iron across global environments, Global Biogeochem. Cy. 36, https://doi.org/10.1029/
580 2022gb007447,2022.
581 Ma, W. W., Zhu, M. X., Yang, G. P., and Li, T.: Iron geochemistry and organic carbon preservation
582 by iron (oxyhydr) oxides in surface sediments of the East China Sea and the south Yellow Sea,
583 J. Marine Syst., 178, 62-74, https://doi.org/10.1016/ j.jmarsys. 2017.10.009,2018.
584 McLeod, E., Chmura, G. L., Bouillon, S., Salm, R., Björk, M., Duarte, C. M., Lovelock, C. E.,
585 Schlesinger, W. H., and Silliman, B. R.: A blueprint for blue carbon: toward an improved
586 understanding of the role of vegetated coastal habitats in sequestering CO_2, Front. Ecol.
587 Environ., 9, 552-560, https://doi.org/10.1890/110004,2011.
588 Meisner, A., Gera Hol, W. H., de Boer, W., Krumins, J. A., Wardle, D. A., and van der Putten, W.H.:
589 Plant–soil feedbacks of exotic plant species across life forms: a meta-analysis, Biol. Invasions,
590 16, 2551-2561, https://doi.org/10.1007/ s10530-014-0685-2,2014.
591 Mu, C. C., Zhang, T. J., Zhao, Q., Guo, H., Zhong, W., Su, H., and Wu, Q. B.: Soil organic carbon
592 stabilization by iron in permafrost regions of the Qinghai-Tibet Plateau, Geophys. Res. Lett.,
593 43, 10, 286-294, https://doi.org/ 10.1002/2016GL070071,2016.
594 Pan, Y. D., Birdsey, R. A., Fang, J. Y., Houghton, R., Kauppi, P. E., Kurz, W. A., et al.: A large and
595 persistent carbon sink in the world's forests, Science, 333, 988-993. https://doi.org/10.1126/
596 science.120160,2011.
597 Patzner, M. S., Mueller, C. W., Malusova, M., Baur, M., Nikeleit, V., Scholten, T., Hoeschen, C.,
598 Byrne, J.M., Borch, T., and Kappler, A.: Iron mineral dissolution releases iron and associated
599 organic carbon during permafrost thaw, Nat. Commun., 11, 1-11, https://doi.org/10.1038/
600 s41467-020-20102-6,2020.
601 Patzner, M. S., Kainz, N., Lundin, E., Barczok, M., Smith, C., Herndon, E., Kinsman-Costello, L.,

602 Fischer, S., Straub, D., Kleindienst, S., Kappler, A., and Bryce, C.: Seasonal fuctuations in iron
603 cycling in thawing permafrost peatlands, seasonal fluctuations in iron cycling in thawing
604 permafrost peatlands. Environ. Sci. Technol., 56, 4620-4631, https://doi.org/10.1021/acs.est.
605 1c06937,2022.
606 Peter, S., and Sobek, S.: High variability in iron-bound organic carbon among five boreal lake
607 sediments, Biogeochemistry, 139, 19-29, https://doi.org/10.1007/ s10533-018-0456-8,2018.
608 Riedel, T., Zak, D., Biester, H., Dittmar, T.: Iron traps terrestrially derived dissolved organic matter
609 at redox interfaces. Proc. Natl. Acad. Sci. USA., 110, 10101-10105, https://doi.org/
610 10.1073/pnas.1221487110,2013.
611 Roulet, N. T.: Peatlands, carbon storage, greenhouse gases, and the Kyoto Protocol: Prospects and
612 significance for Canada, Wetlands, 20, 605-615, https://doi.org/10.1672/0277-5212(2000)020
613 [0605:PCSGGA]2.0.CO;2,2000.
614 Salvadó, J. A., Tesi, T., Andersson, A., Ingri, J., Dudarev, O. V., Semiletov, I. P., Gustafsson, Ö.:
615 Organic carbon remobilized from thawing permafrost is resequestered by reactive iron on the
616 Eurasian Arctic Shelf, Geophys. Res. Lett., 42, 8122-8130, https://doi.org/10.1002/2015
617 GL066058,2015.
618 Schmidt, M. W., Torn, M.S., Abiven, S., Dittmar, T., Guggenberger, G., Janssens, I.A., Kleber, M.,
619 Kogel-Knabner, I., Lehmann, J., Manning, D. A., Nannipieri, P., Rasse, D. P., Weiner, S., and
620 Trumbore, S. E.: Persistence of soil organic matter as an ecosystem property, Nature, 478, 49-
621 56, https://doi.org/10.1038/nature10386, 2011.
622 Shields, M. R., Bianchi, T. S., Gélinas, Y., Allison, M. A., and Twilley, R. R.: Enhanced terrestrial
623 carbon preservation promoted by reactive iron in deltaic sediments, Geophys. Res. Lett., 43,
624 1149-1157. https://doi.org/10.1002/ 2015GL067388,2016.
625 Smale, D.A., Wernberg, T., Oliver, E.C.J., Thomsen, M., Harvey, B.P., and Straub, S.C., et al.:
626 Marine heatwaves threaten global biodiversity and the provision of ecosystem services, Nat.
627 Clim. Change, 9, 306-312. https://doi.org/10.1038/ s41558-019-0412-1,2019.
628 Sowers, T. D., Adhikari, D., Wang, J., Yang, Y., and Sparks, D. L.: Spatial associations and chemical
629 composition of organic carbon sequestered in Fe, Ca, and organic carbon ternary systems,
630 Environ. Sci. Technol., 52, 6936-6944, https://doi.org/ 10.1021/acs.est.8b01158,2018a.

631 Sowers, T. D., Stuckey, J. W., and Sparks, D. L.: The synergistic effect of calcium on organic carbon
632 sequestration to ferrihydrite, Geochem. T., 19, 4 https://doi.org/10.1186/s12932-018-0049-
633 4,2018b.
634 Tipping, E., Rey-Castro, C., Bryan, S. E., and Hamilton-Taylor, J.: Al(III) and Fe(III) binding by
635 humic substances in freshwaters, and implications for trace metal speciation, Geochim.
636 Cosmochim. Ac., 66, 3211-3224, https://doi.org/10.1016/S0016-7037(02)00930-4,2002.
637 Wagai, R., and Mayer, L. M.: Sorptive stabilization of organic matter in soils by hydrous iron oxides,
638 Geochim. Cosmochim. Ac., 71, 25-35, https://doi.org/10.1016/j.gca.2006.08.047,2007.
639 Wan, D., Ye, T. H., Lu, Y., Chen, W. L., Cai, P., Huang, Q. Y.: Iron oxides selectively stabilize plant-
640 derived polysaccharides and aliphatic compounds in agricultural soils, Eur. J. Soil Sci., 70,
641 1153-1163, https://doi.org/10.1111/ejss.12827,2019.
642 Wang, D., Zhu, M. X., Yang, G. P., and Ma, W. W.: Reactive iron and iron-bound organic carbon in
643 surface sediments of the river-dominated Bohai Sea (China) versus the Southern Yellow Sea.
644 J. Geophys. Res-Biogeo., 124, 79-98, https://doi.org/10.1029/2018JG004722,2019.
645 Wang, S., Jia, Y., Liu, T., Wang, Y., Liu, Z., and Feng, X.: Delineating the role of calcium in the
646 large-scale distribution of metal-bound organic carbon in soils, Geophys. Res. Lett., 48,
647 e2021GL092391, https://doi.org/10.1029/2021 GL092391,2021.
648 Wang, Y., Wang, H., He, J.S., and Feng, X.: Iron-mediated soil carbon response to water-table
649 decline in an alpine wetland, Nat. Commun., 8, 1-9, https://doi.org/10.1038/ncomms15972,
650 2017.
651 Ye, C., Huang, W., Hall, S.J., and Hu, S.: Association of organic carbon with reactive iron oxides
652 driven by soil ph at the global scale, Global Biogeochem. Cy., 36, e2021GB007128,
653 https://doi.org/10.1029/2021GB007128,2022.
654 Yu, C., Xie, S., Song, Z., Xia, S., and Åström, M. E.: Biogeochemical cycling of iron (hydr-) oxides
655 and its impact on organic carbon turnover in coastal wetlands: A global synthesis and
656 perspective, Earth-Sci. Rev., 218, 103658, https://doi.org/10.1016/j.earscirev.2021.103658,
657 2021.
658 Zhao, B., Jia, Y., Wu, S., Wei, L., Li, J., Hong, H., Yan, C., Williams, M.A., and Wang, Q.:
659 Preservation of soil organic carbon in coastal wetlands promoted by glomalin–iron–organic

carbon ternary system, Limnol. Oceanogr., 67, S180-S192, https://doi:10.1002/lno.12238,2022.

Zhao, Q., Poulson, S. R., Obrist, D., Sumaila, S., Dynes, J. J., McBeth, J. M., Yang, Y.: Iron-bound organic carbon in forest soils: quantification and characterization, Biogeosciences, 13, 4777-4788, https://doi.org/10.5194/bg-13-4777-2016, 2016.

Zong, M., Lin, C., Li, S., Li, H., Duan, C., Peng, C., Guo, Y. M., and An, R.: Tillage activates iron to prevent soil organic carbon loss following forest conversion to cornfields in tropical acidic red soils, Sci. Total Environ., 761, 143253. https://doi.org/10.1016/j.scitotenv.2020.143253, 2021.

Figure captions

Fig. 1 Global distribution of study sites.

Fig. 2 The Fe-OC content (a), *f*Fe-OC (b), soil pH (c), Fe_d content (d), SOC content (e), and Fe-OC/Fe_d molar ratio (f) in different ecosystems shown in the box-plot. Solid dots indicate outliers, and imaginary points represent observations. Box edges are upper and lower quartiles; central lines are median value; whiskers represent standard error. The differences among terrestrial, wetland and marine ecosystems are illustrated (* $p < 0.05$, ** $p < 0.01$, *** $p < 0.001$).

Fig. 3 Relationships between Fe-OC, *f*Fe-OC and soil properties (soil pH, Fe_d, Fe-OC/Fe_d molar ratio, SOC, clay), climate variables (MAT, MAP) and latitude across global ecosystem types. The line represents the line of best fit for each ecosystem, and the shaded area indicates the 95% confidence interval for the global dataset. In marine ecosystems, the climate variables (MAT, MAP) and soil pH are not shown due to limited data.

Fig. 4 The relative importance of climate variables (MAT, MAP), soil properties (SOC,

683 soil pH, Fe-OC:Fe_d, and Fe_d), and geographical location (i.e., latitude) for Fe-OC and
684 *f*Fe-OC in terrestrial (a, b), marine ecosystems (c, d), and wetlands (e, f) by random
685 forest (RF) analysis. The mean square error (MSE) is used to estimate the importance
686 of these predictors, with higher MSE values indicating more important predictors. In
687 marine ecosystems, the climate variables (MAT, MAP) and soil pH are not shown due
688 to limited data. Ratio: Fe-OC/Fe_d molar ratio. Asterisks show significant differences:
689 *$p < 0.05$, and **$p < 0.01$.

690 **Fig. 5** Frequency distributions of the Fe-OC/Fe_d molar ratio in different ecosystems.
691 The molar ratio of Fe-OC:Fed is used as an indicator of Fe/OC interaction types, which
692 is < 1.0 for adsorption and > 6 for coprecipitation (Wagai and Mayer, 2007; Wang et al.,
693 2017).

694 **Fig. 6** The Spearman correlation analysis results of the Fe-OC, Fe-OC/Fe_d molar ratio
695 (i.e., ratio) and environmental factors (MAT, MAP, pH) in terrestrial (a), marine (b) and
696 wetland ecosystems (c). Asterisks show significant differences: *$p < 0.05$, **$p < 0.01$,
697 and *** $p < 0.001$.

698 **Fig. 7** Schematic representation of drivers, dynamic and patterns of Fe-OC associations
699 in different ecosystem types on global scale. Wetland ecosystem included coastal
700 wetlands and inland wetlands; aquatic ecosystem mainly refers to marine and
701 freshwater ecosystems, but the data of freshwater systems in this study are scarce and
702 dominated by marine systems. Data are averages of different ecosystem types. Different
703 coloured triangles and squares represent SOC molecular diversity. A lower SOC

molecular diversity and concomitant lower contents of Fe-OC (e.g., terrestrial and aquatic ecosystems), whereas higher diversity increases the Fe-OC contents (e.g., wetlands). Meanwhile, there was a significant difference in the proportion of Fe-OC in total SOC (*f*Fe-OC). The asterisk (*) indicates significant differences.

709 **Figure 1**

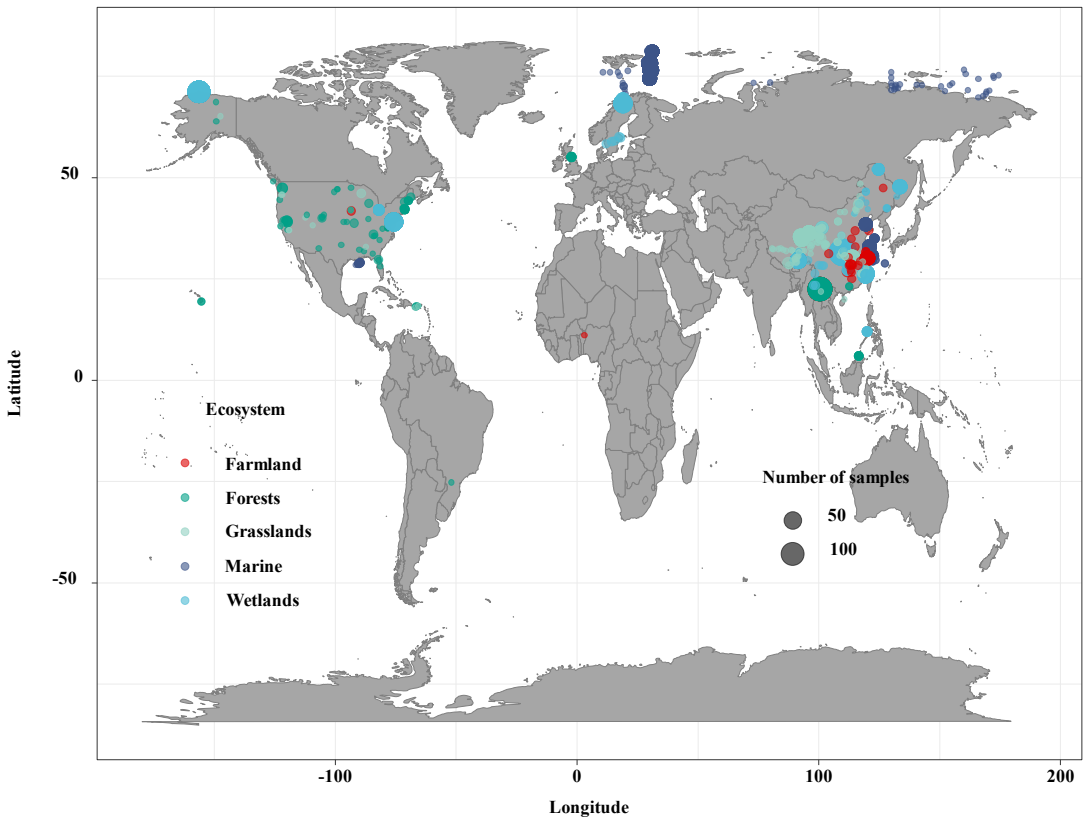

710

711 **Figure 2**

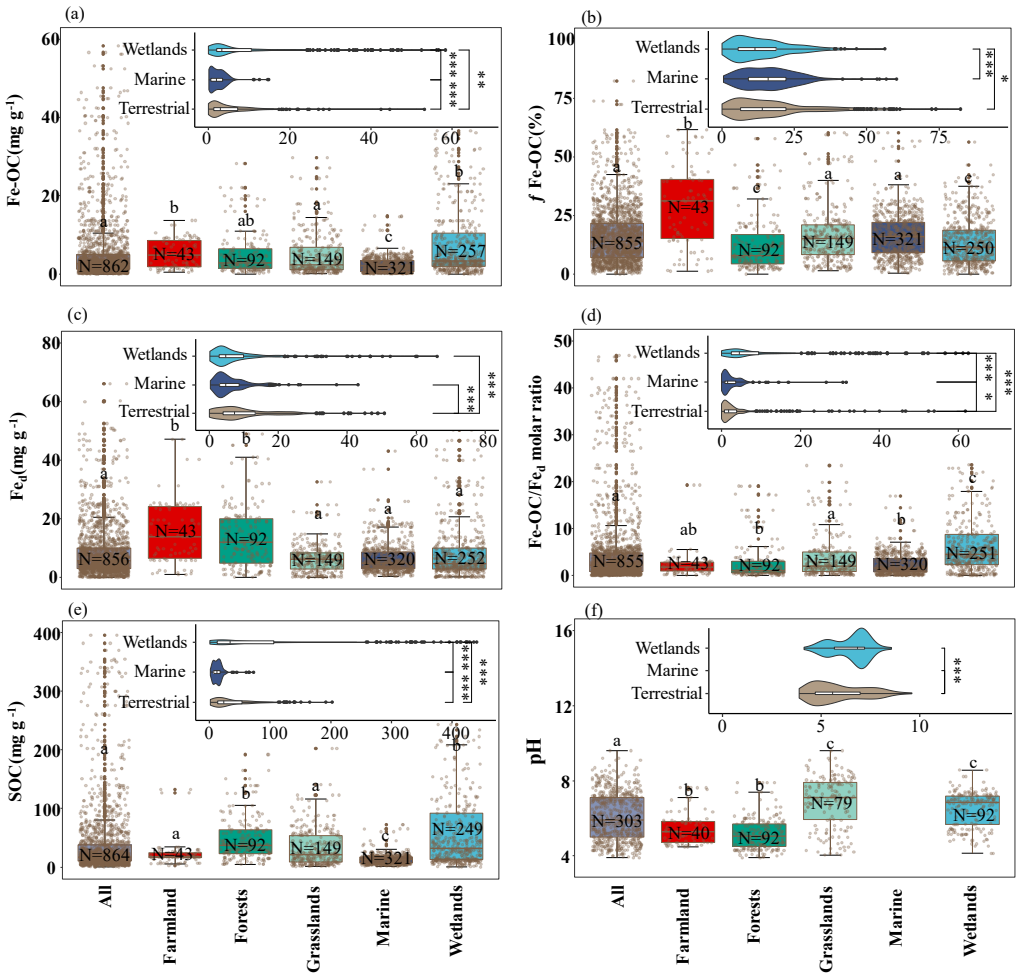

712

713 **Figure 3**

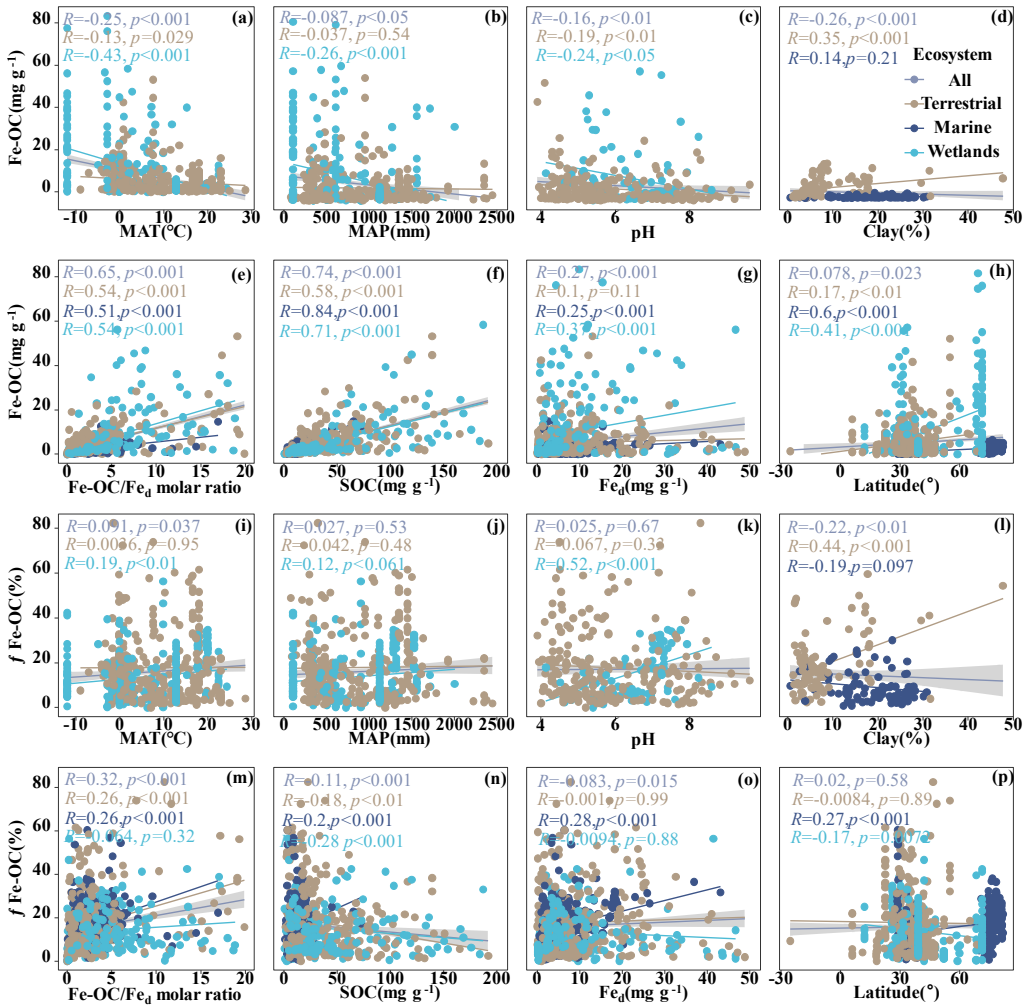

714

715 **Figure 4**

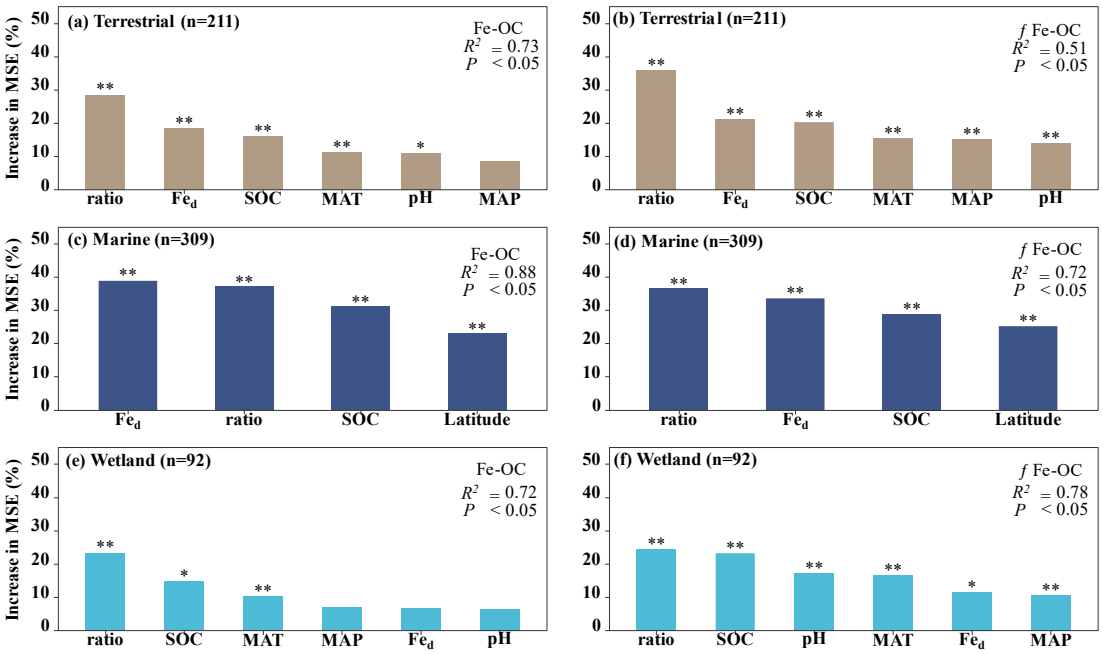

716

717 **Figure 5**

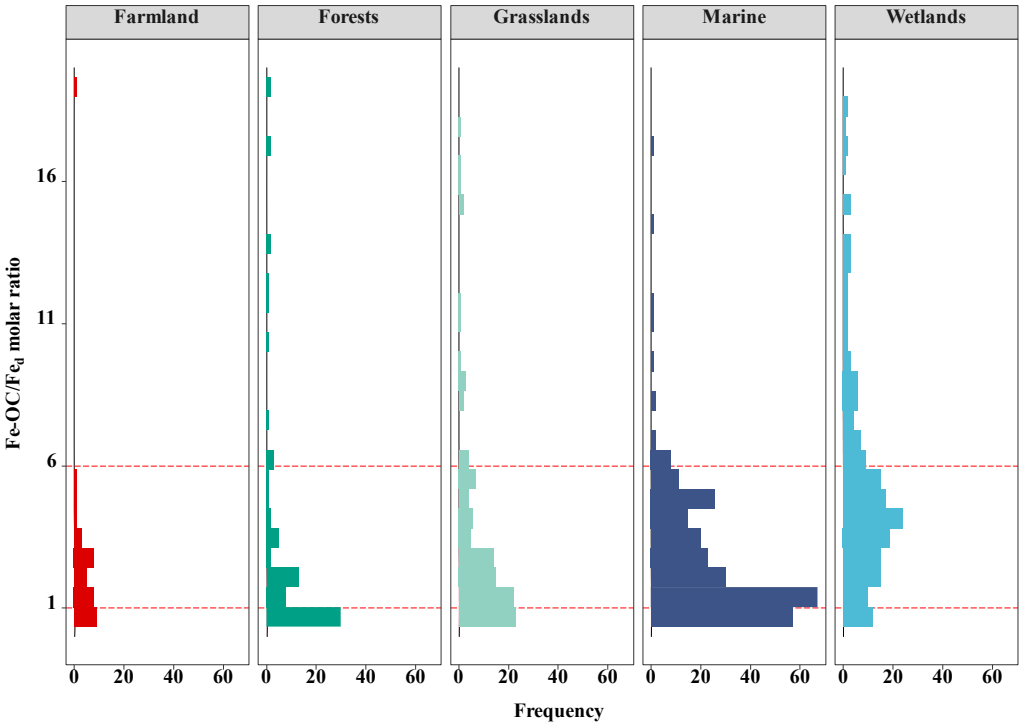

718

719 **Figure 6**

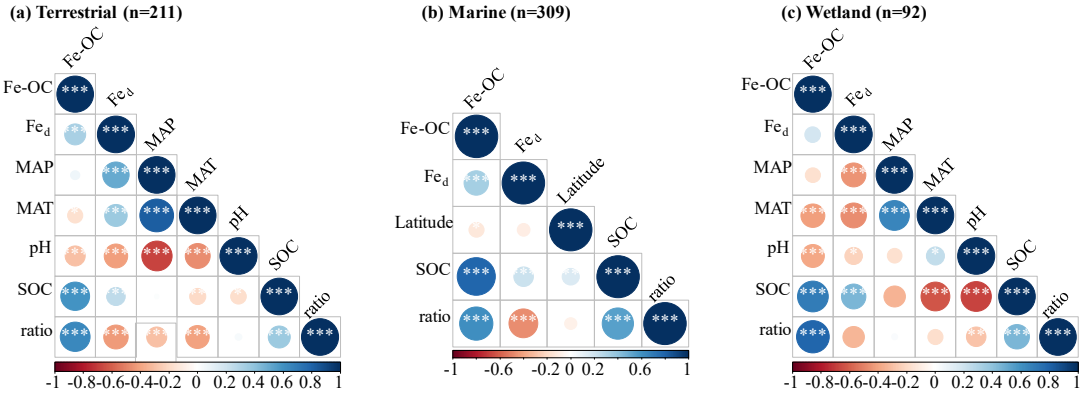

720

721 **Figure 7**

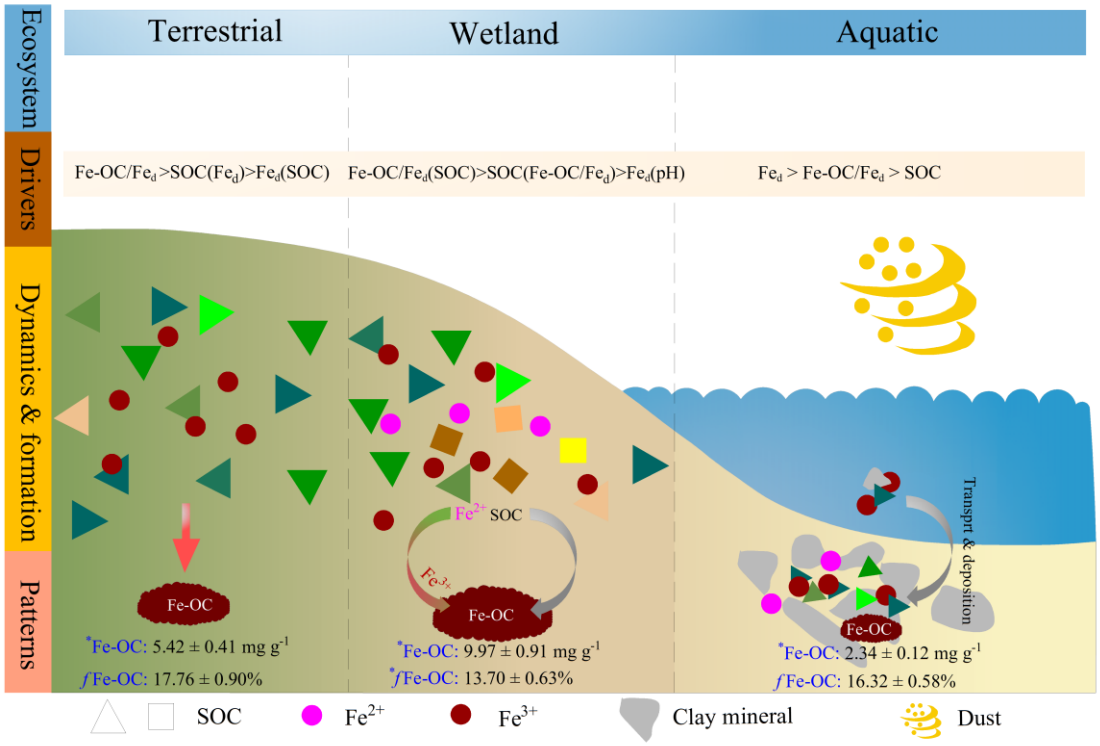

722